

# Chest X-ray image classification using deep belief network with Al-Biruni earth radius and particle swarm optimization

Rakesh Selva Raj<sup>1</sup>, Pavan Kumar Madalu Palakshamurthy<sup>2</sup>, Bidarakere Eswarappa Rangaswamy<sup>3</sup>

<sup>1</sup>Department of Information Science and Engineering, Adichunchanagiri Institute of Technology, JNNCE Shimoga affiliated to Visvesvaraya Technological University, Belagavi, India

<sup>2</sup>Department of Information Science and Engineering, Jawaharlal Nehru New College of Engineering, affiliated to Visvesvaraya Technological University, Belagavi, India

<sup>3</sup>Department of Academics, Visvesvaraya Technological University, Belagavi, India

## Article Info

### Article history:

Received Dec 7, 2024

Revised Oct 27, 2025

Accepted Nov 8, 2025

### Keywords:

Chest X-ray

CLAHE

Deep belief network

Particle swarm optimization

with al-biruni earth radius

SMOTE

## ABSTRACT

Chest X-ray (CXR) is a widely employed radiological clinical assessment tool that provides a quick and effective means of classifying various diseases using CXR images. However, several researchers face challenges with CXR images due to imbalanced datasets and image quality issues. Pre-processing is performed using contrast limited adaptive histogram equalization (CLAHE) to enhance image quality and mitigate noise in the data. The synthetic minority oversampling technique (SMOTE) is applied to create synthetic samples for the minority class and handle class imbalance. The MobileNetV2 performs depth-wise separable convolution is used for feature extraction, while maintaining high efficiency for CXR images. This research proposes a deep belief network (DBN) to classify CXR, which helps capture hierarchical features and complex patterns in CXR images. The combination of particle swarm optimization (PSO) and Al-Biruni earth radius (BER) method is employed for hyperparameter tuning with enhanced DBN classification accuracy. Furthermore, BER is integrated with the PSO algorithm to balance exploration and exploitation while the fitness function is fine-tuned for optimal DBN classification performance. The proposed PSOBER-DBN achieves a high accuracy of 99.86% on the CXR14 dataset, in comparison to existing techniques such as the multi-level residual feature fusion network (MLRFNet).

This is an open access article under the [CC BY-SA](#) license.



## Corresponding Author:

Rakesh Selva Raj

Department of Information Science and Engineering, Adichunchanagiri Institute of Technology

affiliated to Visvesvaraya Technological University

Belagavi, India

Email: rakeshsr.cseng@gmail.com

## 1. INTRODUCTION

Chronic lung disease is a life-threatening condition that occurs due to the collapse of the respiratory system. Increased air pressure in the lungs restricts expansion, resulting in breathing difficulties [1]. Chest X-ray (CXR) play an essential role in detecting a variety of chest diseases affecting organs such as the heart, lungs, and bones. The CXR images are classified using deep learning (DL)-based techniques for enhanced performance with medical images, reducing of image noise, and for alleviating workloads by expediting diagnosis [2], [3]. Expert radiologists manually analyse CXR images to identify marks and signs of the disease. CXR imaging is particularly helpful in diagnosing chest-related diseases like pneumonia and other lung diseases, as it offers a detailed view thoracic cavity [4], [5]. Fourteen classes are used in CXR image classification, but are not balanced, presenting a challenge during neural network training. Data imbalance

causes models to become biased toward majority classes, which impacts overall accuracy. Reducing the size of each class to match the minority class may appear to be a reasonable solution, but it introduces additional problems [6], [7]. The key novelty of this research, setting it apart from other investigations, includes the use of CXR image enhancement DL algorithms, lung feature extraction, activation mapping, and max pooling to connect visualizations and ensure accurate outcomes [8]. Most studies have focused on binary or multi-class classification using CXR images from individuals with various diseases and healthy controls [9]. However, these methods often suffer from limitations that affect classification accuracy [10], [11]. Additionally, certain characteristics of CXR images, such as overlapped organs, blurred boundaries, and low contrast lead to inaccurate diagnoses of pneumonia. These challenges are addressed through image quality enhancement using pre-processing techniques and pre-trained networks, which are commonly applied in various medical imaging tasks [12], [13]. As a result, there is a growing demand for the DL method to assist radiologists in decision-making for enhanced classification accuracy.

In order to address the need for accurate and automatic interpretation of CXR images, numerous studies have employed advanced DL approaches with promising results [14], [15]. Most existing studies suffer from class imbalance and image quality issues due to the limited count of CXR image samples, significantly reducing efficiency of DL classifiers. This research hence proposes a novel particle swarm optimization (PSO) with Al-Biruni earth radius (BER) based on deep belief network (DBN) technique for classification of CXR images with enhanced accuracy. The PSOBER-DBN approach consistently adjusts values and updates population size for identifying the best position. The study considers an account of existing DL algorithms used for CXR image classification, along with their advantages and drawbacks. Shamrat *et al.* [16] presented a fine-tuned MobileLungNetV2 model for the analysis of CXR images through the effective classification of X-ray images using the CXR14 dataset. A lightweight model was deployed for various classes of the CXR to address the need for extensive training from scratch. However, the MobileLungNetV2 struggled to process different types of X-ray images and faced imbalance issues, ultimately affecting classification performance. Li *et al.* [17] implemented multi-level residual feature fusion network (MLRFNet) for image classification using the CXR14 dataset. The model's generated classification vectors enabled the network to incorporate spatial location information for specific diseases in its predictions. However, although MLRFNet incorporated mechanisms to improve generalization, the added complexity from multiple feature fusion layers still led to overfitting, which affected the accuracy.

Jin *et al.* [18] suggested a multi-label classification approach for fine tuning of the convolutional network next (ConvNeXt) network using the CXR14 dataset. Visual vectors were combined with semantic vectors encoded by several features, taking into account relationships through a weighted metric loss between images and labels. However, ConvNeXt features struggled to capture the high dimensionality due to varying dimensions, which affected the classification accuracy. Mezina and Burget [19] developed a neural network for CXR analysis and introduced a specific loss function for multi-label classification, known as the asymmetric loss function (ASL). The neural network with a binary cross-entropy (BCE) loss function was fine-tuned to extract global features at different scales from input images. The challenge with BCE was its sensitivity to minority classes, which led to overfitting, particularly due to its high sensitivity to noise, where false positives and negatives carried different cost implications for risk management. Jin *et al.* [20] introduced a cross-model deep metric learning generalized zero-shot learning (CM-DML-GZSL) method. A weighted focal Euclidean distance loss function was designed to emphasize hard samples, helping the model classify more effectively and achieve higher accuracy. However, the CM-DML-GZSL model's cross-model DL approach and loss function computation introduced significant overhead, which affected overall performance. Irtaza *et al.* [21] considered the various pre-trained methods such as MobileNet, DenseNet, EfficientNet, InceptionV3, VGG-16 and Xception for the multi-label lung disease classification. The target to enhance an effectiveness of those methods through the experimentation by parameter optimization. The MobileNet generated the optimal outcomes as compared to other approaches. The deep convolutional generative adversarial network (GAN) was implemented to generate the synthetic X-ray images which involved diverse pathologies already involves in the selected imbalanced dataset. In the overall analysis, existing techniques suffered from limitations such as class imbalance and image quality issues due to the limited number of CXR image samples, significantly reducing the efficiency of DL classifiers.

The key contribution of this research are:

- This research proposes a PSOBER model for fine-tuning the hyperparameters of the DBN, ensuring that the model is trained with the most effective configuration for improved classification accuracy.
- The PSO and BER are combined to perform hyperparameter tuning and efficient classification with high accuracy. This optimization approach identifies the best position by updating population size and adjusting values based on the iterations.
- The synthetic minority oversampling technique (SMOTE) generates synthetic samples for minority classes for achieving a balanced class distribution and enhance learning from the decision boundary more effectively.

This manuscript is further organized as follows: section 2 details the functioning of the proposed PSOBER-DBN method, while section 3 discusses the results and comparative analysis, and finally, section 4 concludes the study.

## 2. PROPOSED METHOD

In this research, a PSOBER-DBN is used for classifying CXR images which performs effectively due to its architecture, facilitating efficient feature reuse and improved gradient flow. The CXR14 dataset serves as the input, and pre-processing is applied using contrast limited adaptive histogram equalization (CLAHE) to enhance image contrast, making finer details in the X-ray images more visible. Feature extraction is carried out using the MobileNetV2 model, pre-trained on a large-scale dataset, which ensures high computational efficiency. The PSO algorithm is integrated with the BER method to form an optimized parameter tuning strategy, improving the classification accuracy of the DBN. Figure 1 presents the overall workflow of the proposed approach.

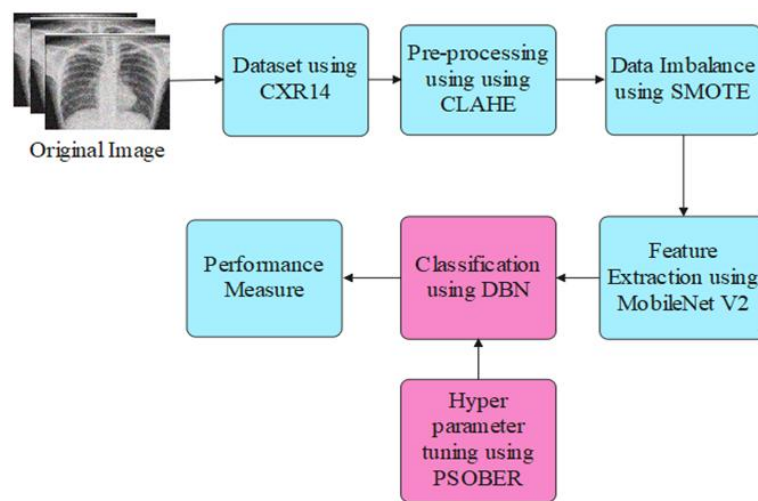


Figure 1. Overall process of proposed method

### 2.1. Dataset description and exploration

The chest X-ray 14 [22] dataset consists of 112,120 frontal CXR images collected from 26,506 patients. All CXR images are presented in PNG format with the dimensions of 1024×1024. The CXRs are labelled with 14 classes of chest X-ray diseases which are as follows: atelectasis, infiltration, pneumothorax, consolidation, emphysema, fibrosis, effusion, pneumonia, pleural thickening, cardiomegaly, nodule, edema, mass, and hernia. The quantities of each disease type are not specified, and the dataset is highly imbalanced, posing a significant challenge for classification. Table 1 presents the training and testing split of the CXR14 dataset.

Table 1. Training and testing of the CXR14 dataset

Name of diseases	No of training image	No of testing image
Atelectasis	3724	843
Cardiomegaly	874	219
Infiltration	7637	1910
Mass	1711	428
Nodule	2164	541
Pneumothorax	1755	439
Consolidation	1048	126
Edema	502	126
Emphysema	714	178
Pneumonia	1194	299
Pleural Thickening	901	225
Fibrosis	582	145
Hernia	88	22
Total	21183	5323

## 2.2. Pre-processing

After data collection, the pre-processing phase addresses contrast and noise issues caused by various interference sources during the imaging process and data acquisition [23]. CLAHE is applied to enhance image contrast by processing small patches independently. Compared to other techniques like adaptive histogram equalization (AHE), CLAHE performs better in local contrast enhancement and effectively limits noise in the image. CLAHE enhances the natural appearance of images by redistributing gray levels within small patches using a user-defined threshold limit. The resulting CLAHE image exhibits a bell-shaped histogram similar to a Rayleigh distribution, whereas histogram equalization (HE) produces a uniform distribution. HE techniques often create saturated regions, while CLAHE provides smooth transitions of intensities between adjacent pixels, enhancing overall image quality. These pre-processed images are then balanced using SMOTE.

## 2.3. Data imbalance using SMOTE

SMOTE [16] is applied to the training data from pre-processed images of the minority class. Initially, images are compressed to create a vector embedding for each image, which is then fed into the SMOTE algorithm. This algorithm uses an arbitrary factor in the latent space of the image to generate synthetic samples. Imbalanced data negatively impacts model quality, so SMOTE selects one or more nearest neighbors from the same class and creates synthetic instances by interpolating between selected instances and their neighbors. This process generates new, similar instances along line segments connecting existing instances in the feature space. The SMOTE approach aims to generate new minority class samples instead of duplicating existing ones. In chest X-ray datasets, certain diseases are underrepresented, leading to class imbalance. This causes the model to be biased toward majority classes, reducing its ability to accurately classify minority class instances. The process iterates until the minority class reaches a proportion similar to that of the majority class. The main goal is to improve classification by setting a maximum class weight for minority classes using weighting techniques. This approach avoids overfitting by generating new artificial samples for minority classes as needed. The balanced CXR images are then fed into feature extraction for classification.

## 2.4. Feature extraction

After balancing the images, essential features are extracted from the balanced CXR images to provide a rich representation for the classification model. MobileNetV2 [24] is used for feature extraction, performing depthwise separable convolutions that reduce computation and the number of parameters while maintaining high efficiency for CXR images. MobileNetV2 is a lightweight convolutional neural network designed for efficient CXR image classification, enabling the model to quickly adapt to new features with improved performance. The goal of feature extraction is to capture relevant features from CXR images to achieve high classification accuracy.

Without feature extraction, more complex models consume significantly more energy, especially when data is limited or insufficiently labeled. Directly processing raw images often leads to poor performance due to lower accuracy and a lack of structured information. MobileNetV2 stands out as a compact deep neural network that reduces model size and computational cost. It incorporates a linear bottleneck layer and an inverted residual block as key components. The linear bottleneck layer replaces the rectified linear unit (ReLU) activation function with a linear function. The core structure of MobileNetV2, known as the bottleneck residual block, uses max pooling to facilitate classification. After applying seven bottleneck residual blocks, the feature layer expands to  $7 \times 7 \times 320$ . A global average pooling operation then reduces the feature dimension from  $7 \times 7 \times 1280$ . Figure 2 illustrates the architecture of the MobileNetV2 model. It provides adjustable parameters for the width and resolution of the input image size, allowing flexibility in processing CXR images. The feature-extracted images are then fed into the classification model for CXR image analysis.

## 2.5. Classification

In this research, the proposed PSOBER-DBN technique employs hyperparameter tuning to optimize the search space by adjusting values to find the best position and updating the population size. The number of iterations is controlled through hyperparameter tuning to enhance classification accuracy. Proper hyperparameter tuning improves model performance on both training and validation datasets and enhances the model's capacity to generalize to unseen data. It optimizes parameters such as learning rate and batch size to accelerate convergence and efficiently utilize computational resources, thereby reducing training time and costs. The PSO-BER approach effectively explores the global search space and avoids local minima. Compared to Bayesian optimization, the proposed method better balances exploration and exploitation, reducing the risk of suboptimal solutions and increasing the likelihood of finding the global optimum.

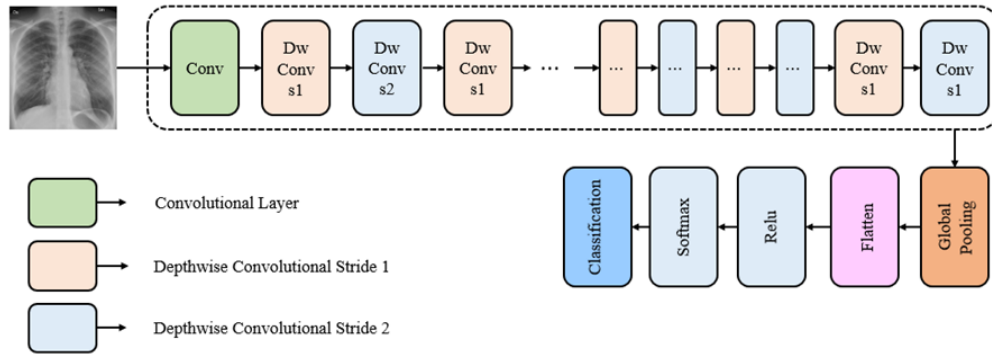


Figure 2. Architecture of MobileNetV2

### 2.5.1. Hyper parameter tuning using PSOPER

Hyperparameter tuning is crucial in CXR image classification to improve efficiency and achieve high accuracy. The PSO and BER techniques are combined to develop a hybrid optimization approach for parameter tuning, enhancing the accuracy of the DBN used in CXR image classification. The PSO algorithm employs a population of particles, each with its own velocity, which are adjusted iteratively. The velocity of the  $n$ th particle as it explores the search space is represented by a D-dimensional vector, as shown in (1). Each particle's personal best position in the solution space is defined as its particular extremum, represented by specific notation. As particles identify both global and local extrema, their current velocity and position are updated, as expressed in (2) to (4).

$$K_n = (K_{n1}, K_{n2}, \dots, K_{nbD}), n = 1, 2, \dots, N \quad (1)$$

$$V_{best} = V_{n1}, V_{n2}, \dots, V_{nbD}, n = 1, 2, \dots, N \quad (2)$$

$$K_n(s+1) = wK_n(s) + c_1r_1(B_p - B_n(s)) + c_2r_2(B^* - B_n(t)) \quad (3)$$

$$K_n(s+1) = K_n(s) + K_n(s+1) \quad (4)$$

Where,  $w$  stands for inertia weight,  $B^*$  denotes the global ideal location, and  $c_1$  and  $c_2$  are learning variables randomly chosen between the range of 0 and 2. Particle velocity is indicated by  $K_{nm}$ , while  $r_1$  and  $r_2$  are arbitrary integers between 0 and 1.

The PSO method is employed in the proposed optimization technique to analyze the search space and enhance exploration. PSO updates the velocity of each particle based on the best position found by the entire swarm, improving the velocity of individual particles accordingly. PSO explores the global search space with a population of particles that move based on their own experience. BER performs exploitation by refining solutions to fine-tune hyperparameters, ensuring the best solutions are accurately identified. Other optimization methods lack the balance between local and global optima that the proposed PSO-BER approach achieves for CXR image classification. Therefore, PSO and BER combined effectively balance exploration and exploitation. The BER method works to find optimal solutions within specified constraints as part of the optimization algorithm. The search space is divided into two groups dedicated to exploration and exploitation, which improves search efficiency. To maintain a balance between exploitative and exploratory pursuits, agents dynamically shift between these subgroups. Increasing the number of agents in both exploration and exploitation groups improves their global average fitness. Before the BER optimization process begins, several parameters must be defined, including the fitness function (FF), which considers the maximum and minimum values allowed in the solution, population size, dimensionality, and the number of solutions. The fitness function evaluates solution quality by considering classification error and the number of selected features, both normalized between 0 and 1. The primary goal is to analyze the BER technique according to (5) to (7).

$$e = h \frac{\cos(y)}{1 - \cos(y)} \quad (5)$$

$$D = e_1(T(s) - 1) \quad (6)$$

$$T(s+1) = T(s) + D(2e_2 - 1) \quad (7)$$

Where,  $0 < \gamma \leq 180$   $h$  is an integer arbitrarily chosen within the interval  $[0,2]$  and the coefficient vectors  $r_1$  and  $r_2$  are those whose values are determined using (13). At iteration  $s$ ,  $T(s)$  represents the solution vector,  $D$  denotes the diameter of the circle, where the search agent searches for promising regions. Equation (8) are applied to formulate the optimal solution.

$$T(s + 1) = r^2(T(t) + D) \quad (8)$$

Where,  $r_3$  is an arbitrary vector calculated using (13). This movement controls the step forward for the best solution,  $T(s)$  represents the solution vector at iteration  $s$ ,  $L(s)$  is a vector denoted by the best solution, and  $D$  represents the distance vector. These components work together to identify the best solution in the surrounding region of the optimal response. Based on the process described above, the BER operates according to (9) and (10). The optimal solution is denoted by  $T^*(s)$ , and it is chosen by first comparing  $T(s + 1)$  and  $T'(s + 1)$ . If the best fitness remains unchanged for two consecutive iterations, the solution undergoes mutation, as expressed in (11).

$$T'(s + 1) = r(T^*(s) + v) \quad (9)$$

$$v = 1 + \frac{2 \times s^2}{Max_{iter}^2} \quad (10)$$

$$T(s + 1) = v * z^2 - h \frac{\cos(x)}{1 - \cos(x)} \quad (11)$$

Where,  $z$  denotes the arbitrary value between  $[0,1]$  and  $t$  represents the number of iterations. The best solution in the BER technique is selected to improve performance, resulting in faster convergence. BER performs exploration or exploitation by adjusting initial parameters such as population size, iteration count, and mutation frequency. These parameters are dynamically modified throughout the iteration process to locate the best solution. The proposed PSOBER algorithm is employed to optimize the parameters of the DBN used for classifying input CXR images. The objective of combining PSO with the BER algorithm is to achieve fast convergence, enhanced exploitation of the search space, and an efficient exploration process. Algorithm 1 outlines the proposed PSOBER algorithm.

#### Algorithm 1. The proposed PSOBER approach

```

Begin BER population  $K_n(n = 1, 2, \dots, e)$  with size  $e$ , iteration  $Max_{iter}$ , fitness function  $F_m, d = 1, m_1, m_2, a, x_1, x_2, x_3, x_4, x_5, x_6, x_1$ .
Evaluate FF  $F_m$  for each  $K_n$ 
Find better solution as  $k^*$ 
While  $d \leq Max_{iter}$  do
  If  $d \% 2 == 0$  then
    For  $(n = 1; i < m_1 + 1)$  do
      Improve  $m$  is referring to Eq. (5)
      Calculate  $D = m_1(T(s) - 1)$ 
      Improve Position to head toward better value as end for
     $P(t + 1) = T(s) + E(2m_2 - 1)$ 
  Stop for
  For  $(n = 1; i < m_2 + 1)$  do
    Evaluate  $E = m_3(L(s) - T(s))$ 
    Update position of better solution as
     $P(t + 1) = m_2(T(s) + E)$ 
    Evaluate is refer to Eq. (10)
    Investigate area around better solution as refer in Eq. (9)
    Compare  $T(s + 1)$  and  $T'(s + 1)$  to choose better solution  $T^*$ 
    If better fitness is not changes for last 2 iteration
      Then
        Solution of mutate as refer in Eq. (11)
      End if
    End if
  End for
  Improve FF  $F_m$  for every  $K(n)$  utilized BER
Else
  Improve FF  $F_m$  for every  $K(n)$  utilized PSO
End if
  Improve BER and PSO parameters,  $n = n + 1$ 
Stop while
Return  $k^*$ 

```

### 2.5.2. PSOBER-DBN using classification

In this research, the DBN technique is employed as a generative probabilistic model consisting of one visible layer and multiple hidden layers that capture statistical correlations among neurons from preceding layers [25], [26]. DBN requires hyperparameter tuning to reduce dimensionality and to improve the exploitation and exploration of the search space, thereby enhancing classification accuracy. As with other deep neural networks, parameter tuning is a critical phase, involving the adjustment of values, population size and related factors to improve model performance. The PSOBER approach, described in the previous section, determines optimal settings for the DBN technique applied to CXR images from the CXR dataset and constructs the classification model accordingly. During the PSOBER phase, parameter tuning involves initializing an arbitrary particle population. Table 2 presents the hyperparameters used for PSOBER.

Table 2. Hyper parameter for PSOBER

Hyper parameter	Range
Learning rate	[0.001 -0.005]
Epochs	[20-40]
Batch size	[30-32]
Amount of RBMs	[3,4,5,6,7]

In the DBN technique, the bias and weight parameters associated with each particle's locations in the population define the characteristics of that particle. The restricted Boltzmann machine (RBM) is trained as a nonlinear classifier using the softmax function to produce a probability distribution over the data labels. The number of hidden units is indicated by  $i$  and  $j$ , corresponding to the input units, where  $m = m_1, m_2, \dots, m_n$ , and  $k = k_1, k_2, \dots, k_n$ . The RBM energy function is described in (12) to (14). In this formulation, nodes in each layer are considered equivalent, but not conditionally dependent, and all layers are distributed accordingly. The function  $R(\theta)$  is used to normalize the input layer under an independent distribution, as defined in (15) to (17).

$$E(k, m; \theta) = -\sum_{h=1}^i \sum_{n=1}^j w_{hn} k_h m_n - \sum_{h=1}^i a_h k_h - \sum_{n=1}^j b_n m_n \quad (12)$$

$$p(k, m) = \frac{1}{R(\theta)} h^{-H(k, m)} \quad (13)$$

$$R(\theta) = \sum_{k, m} h^{-H(k, m)} \quad (14)$$

$$p(k) = \sum_i p(k, m) = \frac{1}{R(\theta)} \sum_m h^{-H(k, m)} \quad (15)$$

$$p(m_n = 1 | k; \theta) = \sigma(\sum_{h=1}^j w_{hn} k_h + b_n) \quad (16)$$

$$p(k_n = 1 | m; \theta) = \sigma(\sum_{h=1}^i w_{hn} m_h + a_h) \quad (17)$$

Where,  $\sigma(x) = \frac{1}{1+\exp(-x)}$  denotes the sigmoid function. By adjusting the biases  $a_h$ ,  $b_n$  and weights  $w_{hn}$ , the RBM aims to maximize the probability  $p(k)$ . The parameter set  $\theta = \{a_h, b_n, w_{hn}\}$  for the RBM is obtained from the training data using a maximum likelihood estimation strategy. The contrastive divergence model is used to estimate this parameter set  $\theta$  using (18) to (20).

$$w_{hn}^{(s+\Delta s)} = w_{hn}^{(s)} + \frac{\alpha}{\beta} (< k_h m_n >_{data} - < k_h m_n >_{model}) \quad (18)$$

$$a_h^{(s+\Delta s)} = a_h^{(s)} + \frac{\alpha}{\beta} (< k_h >_{data} - < k_h >_{model}) \quad (19)$$

$$b_n^{(s+\Delta s)} = b_n^{(s)} + \frac{\alpha}{\beta} (< m_n >_{data} - < m_n >_{model}) \quad (20)$$

After the initial training of the RBM, each subsequent concealed layer is treated as the visible layer for the next RBM in the stack. During the RBM training phase, the costs associated with the population and the optimal individual are progressively improved. Each RBM is initialized arbitrarily to promote diversity within the population.

### 3. EXPERIMENTAL RESULTS

In this research, the PSOBER-DBN technique is simulated in Python environment version 3.8 software tool, with the system specifications being 16 GB RAM, Intel i7 processor, Windows 10 operation system, 16 GB GPU and 1 TB SSD. The performance evaluation and classification results are explained in section 4.1. The effectiveness of the proposed method is assessed using several performance metrics, including accuracy, precision, specificity, F1-score, recall, and area under the curve (AUC). These metrics are defined by (21) to (24).

$$Accuracy = \frac{TP+TN}{TP+TN+FP+FN} \quad (21)$$

$$Precision = \frac{TP}{(TP+FP)} \quad (22)$$

$$Recall = \frac{TP}{TP+FN} \quad (23)$$

$$Specificity = \frac{TN}{TN+FP} \quad (24)$$

$$F1 - Score = \frac{2 \times precision \times Recall}{precision + recall} \quad (25)$$

Where,  $TP$ ,  $TN$ ,  $FP$ , and  $FN$  denote true positive, false positive, false negatives and true negative values, respectively.

#### 3.1. Performance analysis

In this section, the proposed method involving hyperparameters and classification processes is evaluated using several performance metrics, including accuracy, specificity, F1-score, recall, and AUC, as presented in Tables 3 and 4. The performance of feature extraction on the CXR14 dataset is evaluated based on these metrics, as shown in Table 3. Existing approaches such as ResNet-50, VGG-16, EfficientNet and DenseNet are used to compare the performance of feature extraction. The proposed method achieves a high accuracy of 99.86%. MobileNetV2 demonstrates high performance due to its efficient architecture, which combines depth-wise separable convolutions and inverted residuals to reduce computational complexity while maintaining high accuracy.

The classification performance is calculated using various metrics, as presented in Table 4. Existing methods with feature extraction techniques such as ResNet-50, VGG-16, EfficientNet, and DenseNet are evaluated. The proposed method achieves a high accuracy of 99.86%, 97.87% precision, 97.50% recall, 97.58% F1-score, 99.85% specificity and an AUC of 0.897. Figure 3 illustrates the analysis of CXR classes using various metrics. The PSO-BER algorithm optimizes the hyperparameters and structure of the DBN, resulting in improved classification accuracy. Table 4 presents the analysis outcomes of the classification process on the CXR dataset.

Table 3. Analysis of feature extraction process on the CXR dataset

Feature extraction techniques	Accuracy (%)	Precision (%)	Recall (%)	F1 score (%)	Specificity (%)	AUC (%)
ResNet-50	95.59	93.85	95.63	93.09	95.89	0.487
VGG-16	96.96	94.23	96.36	94.23	96.18	0.514
Efficient Net	97.85	95.14	97.86	95.75	97.83	0.635
Dense Net	98.68	96.52	98.36	96.15	98.13	0.795
MobileNetV2	99.86	97.87	97.50	97.58	99.85	0.897

Table 4. Analysis of classification process on the CXR dataset

Classification	Accuracy (%)	Precision (%)	Recall (%)	F1 score (%)	Specificity (%)	AUC
DenseNet201	95.59	93.85	95.63	93.09	95.89	0.487
MLOP	96.96	94.23	96.36	94.23	96.18	0.514
Inception V2	97.85	95.14	97.86	95.75	97.83	0.635
DBN	98.68	96.52	98.36	96.15	98.13	0.795
PSOBER-DBN	99.86	97.87	97.50	97.58	99.85	0.897

Figure 4 presents classification results using different K-fold values for the proposed method on the CXR dataset. Compared to values of 2, 4, and 7, using 5-fold cross-validation ensures that the model is trained on a substantial portion of the data while also validating on a reasonable subset. This balanced approach facilitates better generalization to unseen data, minimizing the risk of overfitting and ensuring sufficient training data to effectively capture underlying patterns.



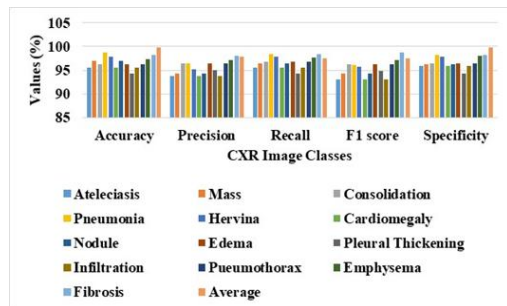


Figure 3. Graphically represented 14 classes on CXR14 dataset

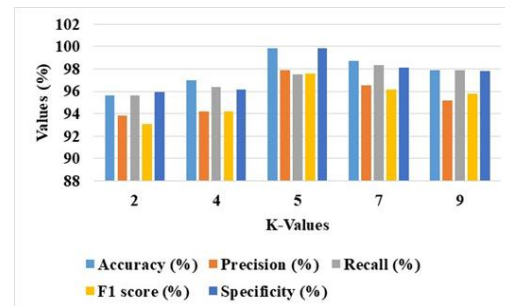


Figure 4. Classification using different K-fold values on the CXR dataset

### 3.2. Comparative analysis

In this section, the proposed PSOBER-DBN technique efficiently classifies CXR images, achieving better accuracy. Table 5 presents the comparative analysis of the proposed PSOBER-DBN method with existing approaches such as MobileLungNetV2 [16], MLRFNet [17], ConvNeXt [18] and BCE [19] on the CXR14 dataset. The proposed PSOBER-DBN method achieves superior performance, attaining an accuracy of 99.86% and an AUC of 0.899 on the CXR14 dataset, outperforming state-of-the-art methods. The superior accuracy of the PSOBER-DBN model is attributed to its combination of PSO with BER and the DBN model. This approach optimizes both the hyperparameters and the structure of the DBN, enhancing its ability to extract meaningful features from CXR images. For better interpretability, the decimal values of existing methods like MLRFNet [17], ConvNeXt [18], and BCE [19] are converted into percentage based on the values of proposed method for better understandability.

Table 5. Comparative analysis of proposed method on CXR14 dataset (NA–Not Available)

Methods	Accuracy	Precision	Recall	F1 score	Specificity	AUC
MLRFNet [17]	N/A	N/A	N/A	N/A	N/A	85.3
ConvNeXt [18]	N/A	N/A	N/A	N/A	N/A	82.6
BCE [19]	73.5	32.16	74.97	42.45	72.21	81.9
ResNet50-V2	93.4	54	55	54.4	98.5	67.4
PSOBER-DBN	99.86	97.87	97.50	97.58	99.85	89.7

### 3.3. Discussion

This section considers the advantages of the proposed approach and the limitations of existing models. The proposed PSOBER-DBN technique is analyzed on the CXR dataset to assess its effectiveness in classifying different diseases from chest X-rays. Initially, pre-processing using CLAHE performs better in local enhancement and reduces noise in the images. The SMOTE approach generates new samples for the minority class, addressing the issue of data imbalance. MobileNetV2, a lightweight convolutional neural network, is designed for efficient CXR image classification, enabling the model to quickly adapt to new features with improved performance. In the final stage, PSO and BER techniques are combined to develop an optimization algorithm that controls parameters and achieves high accuracy in DBN-based CXR image classification. This analysis demonstrates that DBN achieves a high accuracy of 98.62%, outperforming other classifiers. Moreover, the PSOBER-DBN technique shows higher accuracy compared to existing approaches such as MobileLungNetV2 [16], MLRFNet [17], ConvNeXt [18], and BCE [19].

## 4. CONCLUSION

This research proposes the PSOBER-DBN technique for classifying CXR images, aiming to achieve high accuracy by optimizing particle positions and updating the entire population. Initially, data from the CXR dataset is pre-processed using CLAHE, which provides smooth transitions of intensities between adjacent pixels, enhancing image quality. SMOTE generates synthetic samples for minority classes, leading to a more balanced class distribution and enhancing learning near the decision boundary. MobileNetV2 is employed for feature extraction, utilizing depthwise separable convolutions to reduce computation and parameters while maintaining high efficiency for CXR images. The proposed method achieves superior accuracy of 99.86% and 0.899 on the CXR14 dataset, outperforming MobileLungNetV2 and MLRFNet. The implications of this research demonstrate that the PSOBER-DBN technique serves as a robust diagnostic support tool in radiology, assisting clinicians in the early detection of thoracic diseases. Its high accuracy and

adaptability to imbalanced datasets make it suitable for real-world medical applications. Limitations include dependence on a single dataset (CXR14) and a lack of interpretability for clinical decision-making. The model has not yet been validated across diverse medical imaging sources or real-time clinical settings. Future work explores the use of attention-based models (e.g., vision transformers), domain adaptation techniques to generalize across institutions, and explainable AI (XAI) approaches to improve the interpretability of predictions. Additionally, expanding the model's capabilities to multi-modal medical data such as computed tomography (CT) scans and clinical records is investigated.

## FUNDING INFORMATION

Authors state no funding involved.

## AUTHOR CONTRIBUTIONS STATEMENT

This journal uses the Contributor Roles Taxonomy (CRediT) to recognize individual author contributions, reduce authorship disputes, and facilitate collaboration.

Name of Author	C	M	So	Va	Fo	I	R	D	O	E	Vi	Su	P	Fu
Rakesh Selva Raj	✓	✓	✓	✓	✓	✓		✓	✓	✓			✓	
Pavan Kumar Madalu		✓				✓		✓	✓	✓	✓	✓		
Palakshamurthy														
Bidarakere Eswarappa	✓		✓	✓			✓			✓	✓		✓	✓
Rangaswamy														

C : Conceptualization

M : Methodology

So : Software

Va : Validation

Fo : Formal analysis

I : Investigation

R : Resources

D : Data Curation

O : Writing - Original Draft

E : Writing - Review and Editing

Vi : Visualization

Su : Supervision

P : Project administration

Fu : Funding acquisition

## CONFLICT OF INTEREST STATEMENT

Authors state no conflict of interest.

## DATA AVAILABILITY

The dataset generated during the current study is available in the CXR14 repository <https://www.kaggle.com/datasets/purna135/chest-xray-dataset>.




## REFERENCES

- [1] T. Iqbal, A. Shaikat, M. U. Akram, A. W. Muzaffar, Z. Mustansar, and Y. C. Byun, "A hybrid VDV model for automatic diagnosis of pneumothorax using class-imbalanced chest X-rays dataset," *IEEE Access*, vol. 10, pp. 27670–27683, Mar. 2022, doi: 10.1109/ACCESS.2022.3157316.
- [2] H. Liz, J. H.-Tato, M. S.-Montañés, J. Del Ser, and D. Camacho, "Deep learning for understanding multilabel imbalanced chest X-ray datasets," *Future Generation Computer Systems*, vol. 144, pp. 291–306, Jul. 2023, doi: 10.1016/j.future.2023.03.005.
- [3] S. Chatterjee, S. Maity, M. Bhattacharjee, S. Banerjee, A. K. Das, and W. Ding, "Variational autoencoder based imbalanced COVID-19 detection using chest X-ray images," *New Generation Computing*, vol. 41, no. 1, pp. 25–60, Nov. 2023, doi: 10.1007/s00354-022-00194-y.
- [4] V. Ravi, H. Narasimhan, and T. D. Pham, "A cost-sensitive deep learning-based meta-classifier for pediatric pneumonia classification using chest X-rays," *Expert Systems*, vol. 39, no. 7, Mar. 2022, doi: 10.1111/exsy.12966.
- [5] S. Asif, M. Zhao, F. Tang, and Y. Zhu, "A deep learning-based framework for detecting COVID-19 patients using chest X-rays," *Multimedia Systems*, vol. 28, pp. 1495–1513, Mar. 2022, doi: 10.1007/s00530-022-00917-7.
- [6] T. Huang *et al.*, "Deep transfer learning to quantify pleural effusion severity in chest X-rays," *BMC Medical Imaging*, vol. 22, pp. 100, May 2022, doi: 10.1186/s12880-022-00827-0.
- [7] S. Albahli and G. N. A. H. Yar, "AI-driven deep convolutional neural networks for chest X-ray pathology identification," *Journal of X-ray Science and Technology*, vol. 30, no. 2, pp. 365–376, Mar. 2022, doi: 10.3233/XST-211082.
- [8] Y. H. Bhosale and K. S. Patnaik, "PulDi-COVID: Chronic obstructive pulmonary (lung) diseases with COVID-19 classification using ensemble deep convolutional neural network from chest X-ray images to minimize severity and mortality rates," *Biomedical Signal Processing and Control*, vol. 81, Mar. 2023, doi: 10.1016/j.bspc.2022.104445.
- [9] T. Agrawal and P. Choudhary, "FocusCovid: automated COVID-19 detection using deep learning with chest X-ray images," *Evolutionary Intelligence*, vol. 13, no. 4, pp. 519–533, May 2022, doi: 10.1007/s12530-021-09385-2.
- [10] S. Aggarwal, S. Gupta, A. Alhudhaif, D. Koundal, R. Gupta, and K. Polat, "Automated COVID-19 detection in chest X-ray images using fine-tuned deep learning architectures," *Expert Systems*, vol. 39, no. 3, Jun. 2022, doi: 10.1111/exsy.12749.
- [11] G. M. M. Alshmrani, Q. Ni, R. Jiang, H. Pervaiz, and N. M. Elshennawy, "A deep learning architecture for multi-class lung diseases classification using chest X-ray (CXR) images," *Alexandria Engineering Journal*, vol. 64, pp. 923–935, Feb. 2023, doi: 10.1016/j.aej.2022.10.053.




- [12] Z. Mousavi, N. Shahini, S. Sheykhivand, S. Mojtahedi, and A. Arshadi, "COVID-19 detection using chest X-ray images based on a developed deep neural network," *SLAS Technology*, vol. 27, no. 1, pp. 63–75, Feb. 2022, doi: 10.1016/j.slast.2021.10.011.
- [13] G. Celik, "Detection of COVID-19 and other pneumonia cases from CT and X-ray chest images using deep learning based on feature reuse residual block and depthwise dilated convolutions neural network," *Applied Soft Computing*, vol. 133, Jan. 2023, doi: 10.1016/j.asoc.2022.109906.
- [14] H. Malik, T. Anees, and Mui-zzud-din, "BDCNet: Multi-classification convolutional neural network model for classification of COVID-19, pneumonia, and lung cancer from chest radiographs," *Multimedia Systems*, vol. 28, pp. 815–829, Jan. 2022, doi: 10.1007/s00530-021-00878-3.
- [15] M. A. Khan *et al.*, "COVID-19 classification from chest X-ray images: a framework of deep explainable artificial intelligence," *Computational Intelligence and Neuroscience*, vol. 2022, no. 1, Jul. 2022, doi: 10.1155/2022/4254631.
- [16] F. J. M. Shamrat, S. Azam, A. Karim, K. Ahmed, F. M. Bui, and F. De Boer, "High-precision multiclass classification of lung disease through customized MobileNetV2 from chest X-ray images," *Computers in Biology and Medicine*, vol. 155, Mar. 2023, doi: 10.1016/j.compbiomed.2023.106646.
- [17] Q. Li, Y. Lai, M. J. Adamu, L. Qu, J. Nie, and W. Nie, "Multi-level residual feature fusion network for thoracic disease classification in chest X-ray images," *IEEE Access*, vol. 11, pp. 40988–41002, Apr. 2023, doi: 10.1109/ACCESS.2023.3269068.
- [18] Y. Jin, H. Lu, W. Zhu, and W. Huo, "Deep learning based classification of multi-label chest X-ray images via dual-weighted metric loss," *Computers in Biology and Medicine*, vol. 157, May 2023, doi: 10.1016/j.compbiomed.2023.106683.
- [19] A. Mezina and R. Burget, "Detection of post-COVID-19-related pulmonary diseases in X-ray images using vision transformer-based neural network," *Biomedical Signal Processing and Control*, vol. 87, Jan. 2024, doi: 10.1016/j.bspc.2023.105380.
- [20] Y. Jin, H. Lu, Z. Li, and Y. Wang, "A cross-modal deep metric learning model for disease diagnosis based on chest X-ray images," *Multimedia Tools and Applications*, vol. 82, no. 21, pp. 33421–33442, Feb. 2023, doi: 10.1007/s11042-023-14790-7.
- [21] M. Irtaza, A. Ali, M. Gulzar, and A. Wali, "Multi-label classification of lung diseases using deep learning," *IEEE Access*, vol. 12, pp. 124062–124080, 2024, doi: 10.1109/ACCESS.2024.3454537.
- [22] P. C. Mansingh, "Chest X-ray 14 dataset," *Kaggle*. 2022. Accessed: Jun. 2024. [Online]. Available: <https://www.kaggle.com/datasets/pumal35/chest-xray-dataset>
- [23] A. M. Tahir *et al.*, "Deep learning for reliable classification of COVID-19, MERS, and SARS from chest X-ray images," *Cognitive Computation*, vol. 14, no. 5, pp. 1752–1772, Jan. 2022, doi: 10.1007/s12559-021-09955-1.
- [24] H. Firat and H. Üzen, "Detection of pneumonia using a hybrid approach consisting of MobileNetV2 and squeeze-and-excitation network," *Türk Doğa ve Fen Dergisi*, vol. 13, no. 1, pp. 54–61, Mar. 2024, doi: 10.46810/tdfd.1363218.
- [25] N. Geetha and S. J. S. A. Joseph, "Modified densely connected U-Net with improved convolution deep belief network for lung cancer detection on chest X-rays," *International Journal of Intelligent Systems and Applications in Engineering*, vol. 11, no. 9s, pp. 375–384, Jul. 2023.
- [26] Y. Chen, Y. Wan, and F. Pan, "Enhancing multi-disease diagnosis of chest X-rays with advanced deep-learning networks in real-world data," *Journal of Digital Imaging*, vol. 36, no. 4, pp. 1332–1347, 2023, doi: 10.1007/s10278-023-00801-4.

## BIOGRAPHIES OF AUTHORS






**Rakesh Selva Raj**    has more than 13 years of teaching experience. He is working as Assistant Professor in the Department of Information Science and Engineering, Adichunchanagiri Institute of Technology, Chickmagalur. His research interests include data mining, big data, machine learning, networking, and cloud. He has published papers in international/national conferences and journals. He can be contacted at email: [rakeshsr.cseng@gmail.com](mailto:rakeshsr.cseng@gmail.com).



**Pavan Kumar Madalu Palakshamurthy**    has a Ph.D. from Visveswaraya Technological University, Belagavi. He has more than 15 years of teaching experience and has been executing projects in artificial intelligence, machine learning, human behavior analysis, image processing, and computer vision. He is currently working as a Professor in the Department of Information Science and Engineering, Jawaharlal Nehru New College of Engineering, Shimoga. He is an IEEE Senior Member and a Life Member of ISTE. He has various international journal and conference publications with more than 100 citations. He can be contacted at email: [pavankumarmrp@jnnce.ac.in](mailto:pavankumarmrp@jnnce.ac.in).



**Bidarakere Eswarappa Rangaswamy**    presently working as Registrar, Academics, Visveswaraya Technological University, Belagavi. He was the Dean, Research and Development and Professor and Head at Department of Biotechnology, Bapuji Institute of Engineering and Technology, Davangere. He completed his Masters in 1995 and Ph.D. (2001) from Bangalore University. He has obtained higher level Training in Bacteriology and Air sampling techniques from Environmental Diagnostic Laboratory, Florida, USA in 2008 and attended Course on Aerobiology organized by European Aerobiological Association jointly with international aerobiology association (IAA) at Roskilde University Holbaek, Denmark during July 2011. He can be contacted at email: [swamyber@hotmail.com](mailto:swamyber@hotmail.com).